

## New particle accelerations by magnetized plasma shock waves

Cite as: Phys. Plasmas **12**, 102901 (2005); <https://doi.org/10.1063/1.2080520>

Submitted: 02 March 2005 • Accepted: 31 August 2005 • Published Online: 10 October 2005

Satoshi Takeuchi



View Online



Export Citation

### ARTICLES YOU MAY BE INTERESTED IN

[Electron acceleration by lower hybrid waves in magnetic reconnection regions](#)

Physics of Plasmas **12**, 102110 (2005); <https://doi.org/10.1063/1.2080567>

[Field-aligned accelerations by plasma shocks propagating through interstellar magnetic fields](#)

Physics of Plasmas **19**, 070703 (2012); <https://doi.org/10.1063/1.4736955>

[Carrier capture before entering into a semiconductor quantum dot as a dominant pathway for the reduction of emission efficiency](#)

Journal of Applied Physics **98**, 073709 (2005); <https://doi.org/10.1063/1.2081108>

## Physics of Plasmas

**Special Topic:** Plasma Physics  
of the Sun in Honor of Eugene Parker

Submit Today!



# New particle accelerations by magnetized plasma shock waves

Satoshi Takeuchi<sup>a)</sup>

*Ecosocial System Engineering, University of Yamanashi, 4-3-11 Takeda, Kofu, Yamanashi 400-8511, Japan*

(Received 2 March 2005; accepted 31 August 2005; published online 10 October 2005)

Three mechanisms concerning particle accelerations are proposed to account for the high energy of cosmic rays. A model of magnetized plasma clouds is used to simulate a shock-type wave. The attainable energies of test particles colliding with the moving magnetic clouds are investigated by analytical and numerical methods for the three mechanisms. The magnetic trapping acceleration is a new type of particle trapping and acceleration in which, in principle, the test particle is accelerated indefinitely; hence, this mechanism surpasses the Fermi-type acceleration. In the single-step acceleration, the test particle obtains a significant energy gain even though it only experiences a single collision. Lastly, there is the bouncing acceleration by which the test particle is substantially accelerated due to repeated collisions. © 2005 American Institute of Physics.

[DOI: [10.1063/1.2080520](https://doi.org/10.1063/1.2080520)]

## I. INTRODUCTION

Ultrahigh-energy cosmic rays (UHECR) could experience accelerations anywhere in the dynamic universe. Recent observations have reported<sup>1–3</sup> events in which UHECR have energies exceeding  $10^{20}$  eV. To account for these origins or the ultrahigh energy of particles, many conventional or novel mechanisms<sup>4–6</sup> of particle acceleration in the universe have been presented. However, the nature of the sources that generate such energies remains a mystery.

The second-order Fermi<sup>7</sup> acceleration has been regarded as a typical theory of particle accelerations in the universe. In this theory particles collide stochastically with moving plasma clouds that transport “frozen-in” magnetic fields through interstellar space. Cosmic-ray particles having head-on collisions with such plasma clouds will gain energy, while those having overtaking-type collisions will lose energy. However, on an average, the head-on collisions occur more frequently, so that particles involved in these collisions will gain a net energy through multiple collisions. On the other hand, first-order Fermi acceleration<sup>8–11</sup> proposed in the late 1970s was a more efficient type of acceleration. In that case, particles are accelerated by a strong shock wave propagating through interstellar space. The Fermi acceleration is also known as the diffusive acceleration<sup>12,13</sup> having an energy spectrum with an power-law index of 2.

These Fermi/diffusive acceleration mechanisms would be plausible candidates for the explanation of high-energy particle generation in supernova remnants (SNR),<sup>14</sup> gamma-ray burst (GRB),<sup>15</sup> or active galactic nuclei (AGN).<sup>16</sup> Nevertheless, these mechanisms are too slow and too inefficient to account for the existence of UHECR with an energy exceeding  $10^{18}$  eV. Hence, another mechanism is needed to go beyond the Fermi mechanism.

The magnetic trapping acceleration (MTA) mechanism proposed here is a new type of particle trapping and acceleration. An especially attractive feature of MTA is that, in

principle, the energy gain of the particle is indefinite. The idea of MTA (Refs. 17–20) was first proposed by the author, who used an electromagnetic plane wave with linear polarization as the driving wave to accelerate the particles. In the present case, the driving wave is the more realistic-shock-type wave. This wave plays an important role in generating energetic particles in the universe. Although the MTA approach to UHECR is quite different from Fermi’s theory, there is a definite correspondence between them. Other types of acceleration also are derived from modifications of the MTA mechanism.

## II. MODEL OF MAGNETIZED CLOUD AND BASIC EQUATIONS

Plasma consists of perfectly charged gases in a quasineutral state and as such is confinable by magnetic fields, and vice versa. The main dynamics of plasma is that of sustaining its electric and magnetic fields. Therefore, the plasma cloud of interest here is assumed to carry its frozen-in magnetic field through the interstellar magnetic field (IMF)  $\mathbf{B}_0$ . Let us focus our attention on the electric and magnetic fields in this idealized plasma.

Suppose that a magnetized plasma cloud expands uniformly in the  $xz$  plane, while moving along the  $y$  direction with velocity  $v_p$ . The magnetic-field profile of this cloud, which is moving like a shock wave derived from the Korteweg-de Vries-Burgers (KdVB) equation,<sup>21</sup> can be described by the expression

$$\mathbf{B}_1 = B(y, t) \hat{z} = \frac{B_1}{2} \{-\tanh[k(y - v_p t)] + 1\} \hat{z}, \quad (1)$$

where  $B_1$  is the amplitude of the field. The quantity  $2/k$  corresponds to a longitudinal width of the wave front and  $\hat{z}$  is the unit vector. The electric-field component of the moving cloud is derived from Faraday’s law of induction, which gives

<sup>a)</sup>Electronic mail: [take@yamanashi.ac.jp](mailto:take@yamanashi.ac.jp)

$$\mathbf{E}_1 = -\frac{v_p}{c}B(y,t)\hat{x}, \quad (2)$$

where  $c$  is the velocity of light and  $\hat{x}$  is the unit vector.

The relativistic equation of motion of a test particle interacting with this magnetic cloud is given by

$$m\frac{d\gamma\mathbf{v}}{dt} = q\mathbf{E}_1 + \frac{q}{c}\mathbf{v} \times (\mathbf{B}_1 + \mathbf{B}_0), \quad (3)$$

where  $m$  and  $q$  are the mass and charge, respectively, of the particle, and where  $\gamma$  is the Lorentz factor defined by  $\gamma \equiv 1/\sqrt{1-(\beta_x^2 + \beta_y^2 + \beta_z^2)}$ . We consider the case where the direction of the uniform magnetic field  $\mathbf{B}_0 = -B_0\hat{z}$  is opposite to that of the magnetic field of the moving cloud. Therefore, the equation of motion can be written in component form,

$$m\frac{d\gamma v_x}{dt} = -\frac{qv_p}{c}B(y,t) + \frac{q}{c}v_y[B(y,t) - B_0], \quad (4)$$

$$m\frac{d\gamma v_y}{dt} = -\frac{q}{c}v_x[B(y,t) - B_0]. \quad (5)$$

Since the quantities in the  $z$  direction are uniform, we can neglect the corresponding component without loss of generality. The energy equation associated with the particle motion is found by integration to be

$$mc^2\frac{d\gamma}{dt} = -\frac{qv_p v_x}{c}B(y,t). \quad (6)$$

### III. MAGNETIC TRAPPING ACCELERATION

Now, consider the force acting on the particle in the rest frame of the moving cloud. For this purpose, we define new variables,  $Y = y - v_p t$  and  $V_y = v_y - v_p$ . It follows from Eqs. (5) and (6) that the particle comoving with the cloud experiences the force

$$F_y \equiv m\frac{d\gamma V_y}{dt} = -q\beta_x \left[ \frac{B(Y)}{\gamma_p^2} - B_0 \right], \quad (7)$$

where  $\beta_x = v_x/c$ . The maximum value of  $B(Y)$  is  $B_1$ . When the first term in the square bracket is greater than the second term, i.e.,  $\max[B(Y)] = B_1 > \gamma_p^2 B_0$ , then a magnetic neutral sheet (MNS) is created at the front surface of the moving magnetic cloud and the IMF. A typical trajectory of the trapped particle is superimposed on the figure. Suppose that the test particle is located near the MNS. This particle feels the Lorentz force due to  $(q/c)\mathbf{v}_p \times \mathbf{B}_0$  and is accelerated in the negative  $x$  direction. Note that the direction of acceleration is perpendicular to that of the moving cloud. The particle having the velocity  $\mathbf{v}_x$  experiences (a) the restoring force generated by the term  $(q/c)\mathbf{v}_x \times (\mathbf{B}_1 + \mathbf{B}_0)$ , and (b) a constant transverse electric field in the negative  $x$  direction. The field of the shock wave accelerates the particle and both its velocity  $\mathbf{v}_x$  and the restoring force increase as time elapses. As a result, once the particle is trapped in the MNS, it can never escape from being accelerated along the sheet. The trapping mechanism presented here is similar to that of

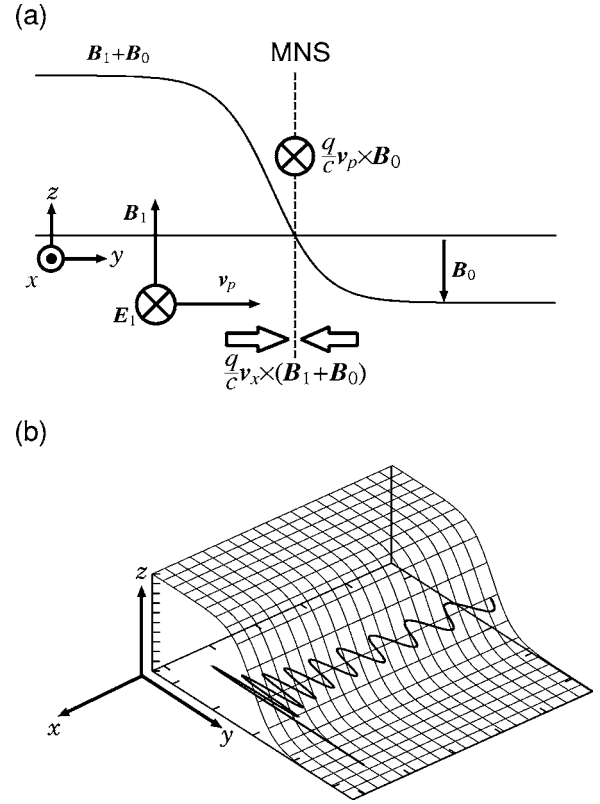


FIG. 1. Schematic diagram of MTA. (a) The test particle comoving with the wave experiences the force  $(q/c)\mathbf{v}_p \times \mathbf{B}_0$  and is accelerated in the negative  $x$  direction. This particle is trapped in the vicinity of the MNS due to the restoring force  $(q/c)\mathbf{v}_x \times (\mathbf{B}_1 + \mathbf{B}_0)$ . This force increases as the particle is accelerated along MNS. (b) A bird's eye view of the shock frame, in which the particle trajectory, superimposed on the magnetic-field profile, shows the meandering motion near the MNS.

meandering motions<sup>22,23</sup> in a stationary MNS.

Integrating Eq. (4) with respect to time, we obtain

$$\gamma\beta_x = \gamma_0\beta_{x0} - \beta_p\Omega t + \frac{q}{mc^2} \int_{\varepsilon} B(Y) - B_0 dY, \quad (8)$$

where  $\gamma_0$  is the initial gain,  $c\beta_{x0}$  the initial transverse velocity, and  $\Omega \equiv qB_0/mc$  the cyclotron frequency. The effect of the integral term in this equation is negligible, because for a tightly trapped test particle the domain  $\varepsilon$  of the integral is reduced by the vanishing of  $B(Y) - B_0$  near MNS. Thus, by the use of the Lorentz factor, the trapped particle with  $\beta_y \approx \beta_p$  obtains the (energy) gain  $\gamma$  and the transverse component  $\beta_x$  given by

$$\gamma = \gamma_p \sqrt{1 + (\gamma_0\beta_{x0} - \beta_p\Omega t)^2} \approx \gamma_p\beta_p\Omega t, \quad (9)$$

$$\beta_x = \frac{\gamma_0\beta_{x0} - \beta_p\Omega t}{\gamma_p \sqrt{1 + (\gamma_0\beta_{x0} - \beta_p\Omega t)^2}} \approx -\frac{1}{\gamma_p}, \quad (10)$$

where the approximations given in these expressions are applicable as time elapses.

In addition, by expanding the magnetic field  $B(Y)$  in Eq. (7) with respect to its position around the MNS, and by making use of the above approximations, we obtain the differential equation of the particle trajectory in the form

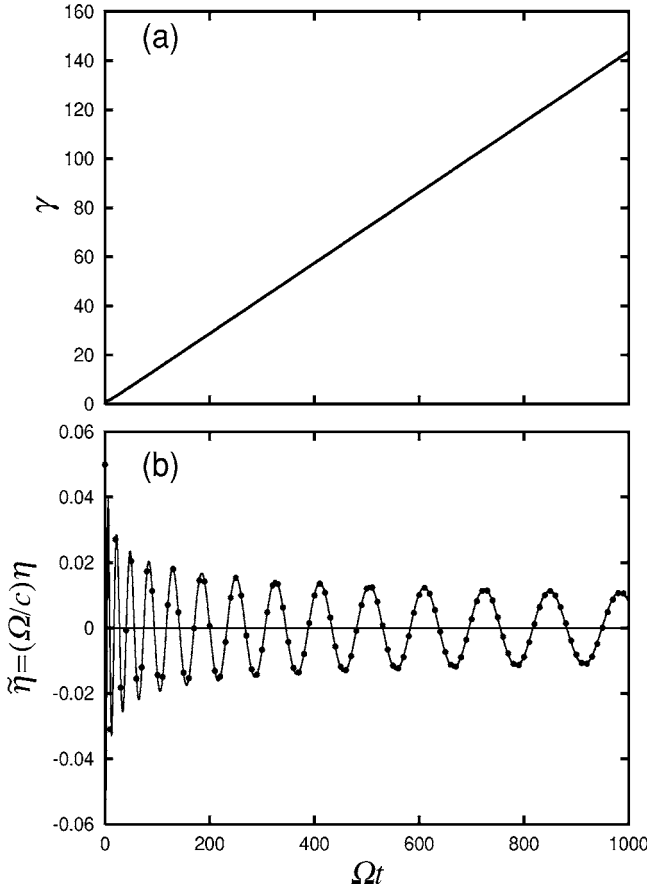


FIG. 2. Time history of the typical (energy) gain and trajectory in MTA. (a) The (energy) gain of the trapped particle increases linearly as time elapses. (b) The dots show the values obtained by numerical calculations, while the solid line is the zeroth-order Bessel function, i.e.,  $\eta = AJ_0(\alpha\sqrt{t})$ , where  $A = 0.13$  is an initial ( $t=0$ ) value, which is a factor of 2 larger than the value used in the numerical calculations.

$$\frac{d^2\eta}{dt^2} + \frac{1}{t} \frac{d\eta}{dt} + \frac{\alpha^2}{4t} \eta = 0, \quad (11)$$

where  $\eta = Y - Y_0$ ,  $Y_0$  is the position of the MNS, and  $\alpha^2/4 = (2kc/B_1\beta_p)(B_1/\gamma_p^2 - B_0)$ . If the condition  $B_1 > \gamma_p^2 B_0$  is satisfied, then  $\alpha$  is a real number, and the solution of the differential equation is given by the zeroth-order Bessel function  $J_0(\alpha\sqrt{t})$ . This means that the trajectory of the trapped particle gradually converges to the MNS as time elapses. The (energy) gain and the particle trajectory are shown in Fig. 2 as a function of time. On the other hand, if  $B_1 < \gamma_p^2 B_0$ , then  $\alpha$  becomes a complex number and the solution is given by the modified Bessel function  $I_0(\alpha\sqrt{t})$ . In that case, the particle travels away from the MNS as time elapses.

We now summarize some of the features of MTA. (a) The moving magnetic cloud propagates perpendicularly to IMF; (b) the effective MNS is created on the wave front of the moving cloud, providing the condition  $B_1 > \gamma_p^2 B_0$  is satisfied; (c) the particle comoving with the cloud can be trapped in the vicinity of the wave front; (d) once the particle is trapped in the MNS, it can never escape and is accelerated indefinitely; (e) the direction of acceleration is along the wave front, that is, perpendicular to the directions of propagation and the direction of the field  $B_0$ ; (f) the energy gain of

TABLE I. Elapsed times and acceleration lengths to achieve UHECR. The acceleration length corresponds to the width of the wave front. The typical scale length of the galaxy size is about 0.01 Mpc.

$G$ ( $10^{20}$ eV)	$t_e$ (s)	$t_e$ (yr)	$l_a$ (Mpc)
$10^{-2}$	$2.0 \times 10^{11}$	$6.3 \times 10^3$	$1.8 \times 10^{-3}$
$10^0$	$2.0 \times 10^{13}$	$6.3 \times 10^5$	$1.8 \times 10^{-1}$
$10^2$	$2.0 \times 10^{15}$	$6.3 \times 10^7$	$1.8 \times 10^1$

the trapped particle increases linearly with time; and (g) this mechanism works effectively not only for electrons, but also for ions corresponding to accelerations being opposite in direction. Similar acceleration mechanisms are presented in the Appendix.

The typical features (d) and (f) are clearly established by analytical methods, however, an indefinite acceleration in a finite universe is not very realistic, even if the theoretical treatment is correct. Hence, we can only estimate the elapsed time  $t_e$  and the acceleration length  $l_a$  of particles that are accelerated to ultrahigh energies. Note that the length  $l_a$  corresponds to a transverse width of the magnetized plasma cloud. The average value of the uniform magnetic field in the universe is given as  $B_0 = 1 \mu\text{G}$ , which clearly satisfies the trapping condition. With the energy gain given by  $G$ , the elapsed time and the acceleration length are obtained from Eqs. (9) and (10), respectively, as

$$t_e = \frac{G}{\gamma_p \beta_p |q| c B_0} = 1.1 \times 10^{13} \frac{G(10^{20} \text{ eV})}{\gamma_p \beta_p B_0(\mu\text{G})} \text{ s}, \quad (12)$$

$$l_a = \frac{ct_e}{\gamma_p} = 1.1 \times 10^{-1} \frac{G(10^{20} \text{ eV})}{\gamma_p^2 \beta_p B_0(\mu\text{G})} \text{ Mpc}. \quad (13)$$

It is found that these values of  $t_e$  and  $l_a$  are independent of particle species. As the speed of the moving cloud and/or the uniform magnetic field increases, the values of  $t_e$  and  $l_a$  are reduced, thus favoring the acceleration. It has been suggested that some UHECR have energies exceeding the Greisen-Zatsepin-Kuz'min (GZK) cutoff<sup>24</sup> ( $\approx 10^{19.5}$  eV). Therefore, for concreteness, let us substitute energy values near the GZK cutoff into Eqs. (12) and (13). For example, assuming that the cloud moves at half the speed of light, i.e.,  $\beta_p = 0.5$  and  $\gamma_p = 1.15$ , we obtain reasonable results for the elapsed time and acceleration length as shown in Table I. We predict that UHECR with energies exceeding  $10^{20}$  eV can be generated over a mean distance scale of galaxy size.

#### IV. ADDITIONAL ACCELERATION MECHANISMS

Using the electromagnetic field configuration of the MTA mechanism, we can investigate other types of particle acceleration. Substituting  $B(y, t)$  from Eq. (6) into Eq. (5), and integrating the latter with respect to time, we arrive at Eq. (15). Equation (14) is a reformulation of Eq. (8),

$$\gamma \beta_x - \gamma_0 \beta_{x0} + \frac{\Omega}{c} (y - y_0) = \frac{q}{mc^2} \int B(Y) dY, \quad (14)$$



$$\gamma\beta_y - \gamma_0\beta_{y0} - \frac{\Omega}{c}(x - x_0) = \frac{1}{\beta_p}(\gamma - \gamma_0). \quad (15)$$

Under the conditions of the tight-particle trapping, i.e.,  $y - y_0 = v_p t$ ,  $x - x_0 = -ct/\gamma_p$ , and  $B(Y) = 0$ , Eqs. (14) and (15) lead to Eqs. (9) and (10), respectively.

### A. Single-step acceleration

Consider first the case where the uniform magnetic field is nonexistent. This case is almost the same as that corresponding to a particle being accelerated by a relativistic blast wave<sup>25–27</sup> propagating in vacuum. If the uniform magnetic field vanishes, i.e.,  $\Omega = 0$ , then Eqs. (14) and (15) can be written as

$$\gamma\beta_x = \gamma_0\beta_{x0} + \frac{q}{mc^2} \int_0^\infty B(Y) dY \approx \gamma_0\beta_{x0} \quad (16)$$

and

$$\gamma\beta_y = \gamma_0\beta_{y0} + (\gamma - \gamma_0)/\beta_p, \quad (17)$$

respectively. The definite integral with respect to  $Y$  differentiates this case from that in which the uniform magnetic field exists. Suppose that a test particle approaches the magnetic cloud from an indefinite distance and collides with the wave front. During the collision, the particle gains momentum as it is reflected perfectly by the magnetic field. After the collision it escapes from the cloud and runs away to some other indefinite distance. Consequently, the contribution of the integral term becomes negligibly small.

Using the definition of  $\gamma$ , we can eliminate the variables  $\beta_x$  and  $\beta_y$  from Eqs. (16) and (17). Therefore, the net gain  $\Delta\gamma \equiv \gamma - \gamma_0$  is expressed entirely in terms of known quantities as

$$\frac{\Delta\gamma}{\gamma_0} = \frac{2\beta_p(\beta_p - \beta_{y0})}{1 - \beta_p^2} = 2\gamma_p^2\beta_p(\beta_p - \beta_{y0}), \quad (18)$$

where  $\gamma_p = (1 - \beta_p^2)^{-1/2}$  is the Lorentz factor of the relativistic shock wave. The head-on collision occurs when the initial value  $\beta_{y0}$  is negative, and then the particle gains net energy. On the other hand, if  $\beta_{y0}$  is positive, then the particle loses energy due to the overtaking-type collision. Some features of this acceleration are described as follows: The head-on collision between the particle and the cloud occurs only once; in addition, the increasing rate of net gain  $\Delta\gamma$  depends on the speed of the magnetic cloud, i.e.,  $\Delta\gamma/\gamma_0 \approx 2\beta_p|\beta_{y0}|$  with  $\beta_p < |\beta_{y0}| < 1$ , and this is comparable to first-order Fermi acceleration with  $\Delta\gamma/\gamma_0 \approx \beta_p$ . Furthermore, if  $\beta_p \approx 1$  is satisfied, then we obtain  $\Delta\gamma/\gamma_0 \approx 2\gamma_p^2(1 - \beta_{y0})$ . This characterization of the single-step acceleration is quite different from that of the Fermi acceleration. Consequently, as the speed of the magnetic cloud approaches the speed of light, namely, that of the ultrarelativistic blast wave, the energy gain increases dramatically as shown in Fig. 3. However, the acceleration efficiency is substantially small because of the single-step acceleration. The results obtained here are also derived from the head-on reflection between a ball and a wall moving with a relativistic velocity  $c\beta_p$ .

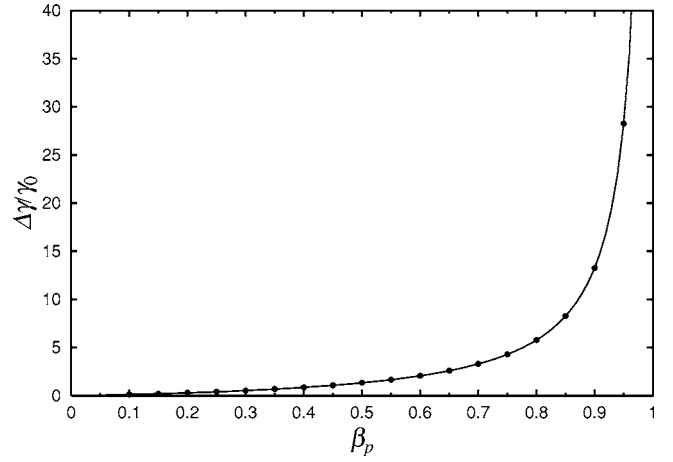


FIG. 3. The rate of (energy) gain obtained through the head-on collision in the single-step acceleration. The transverse axis shows the speed of the moving cloud. As the speed approaches the velocity of light ( $\beta_p = 1.0$ ), the (energy) gain after the collision increases dramatically. The series of dots shows the values obtained by numerical calculations and the solid line is the analytical result given by Eq. (18) where  $\beta_{y0} = 0.5$  is used.

### B. Bouncing acceleration

Let us return to the case of the uniform magnetic field  $\mathbf{B}_0$  and assume that the polarizations of the two magnetic fields are the same. In this case the MNS is not created; hence, an effective acceleration can never be expected. However, if the condition  $|\mathbf{B}_0| \ll |\mathbf{B}_1|$  is satisfied, the particle behaves in an attractive manner. As time elapses, the motion of the test particle is categorized in three stages depending upon the magnitude of the field  $\mathbf{B}_1 + \mathbf{B}_0$ . The left-hand sides of Eqs. (14) and (15) describe the cyclotron motion in the uniform magnetic field  $\mathbf{B}_0$ , whereas the right-hand sides show the influence of the moving magnetic cloud. If the particle initially exists in the region of the uniform magnetic field  $\mathbf{B}_0$ , then it stays there with a cyclotron motion until the magnetic cloud approaches, i.e.,  $B(Y) = 0$  and  $\gamma = \gamma_0$ . At the next stage, the magnetic cloud begins to affect the particle's motion. In the first collision, the rate of net gain of the particle is given approximately by Eq. (18) of the single-step acceleration discussed previously. After multiple collisions, the particle gains net energy. Explicit formulas for such a nonlinear phenomenon are difficult to achieve; hence, the energy gain and a typical trajectory of the particle in the rest frame of the cloud is shown numerically in Fig. 4. Finally, the particle riding on the shoulder of the magnetic cloud falls behind the wave front with a drifting motion, i.e.,  $\int B(Y) dY \approx B_1 Y = B_1(y - v_p t)$ . As a result, the particle gains net energy through many collisions; however, the efficiency of particle acceleration is not very high because of the finite collision times.

## V. CONCLUSIONS

By means of the MTA mechanism, charged particles are selectively accelerated perpendicularly to the IMF, thereby making this mechanism is quite unique. The model presented here is that of an electromagnetic wave which propagates like a shock wave across the IMF. The magnitude of the

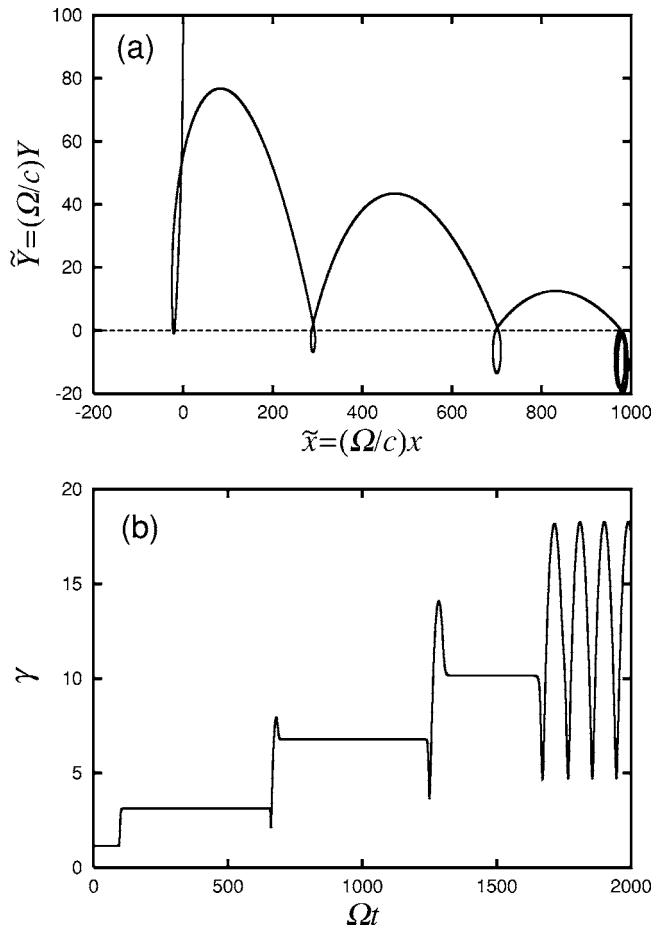


FIG. 4. The (energy) gain and trajectory of the particle in the bouncing acceleration. (a) A typical trajectory of the particle is depicted in the wave frame, in which the particle has multiple collisions with the moving cloud and finally falls behind the wave front. Note that the longitudinal axis indicates the position of the particle in the rest frame of the moving cloud. The dotted line shows the wave front. (b) The particle obtains a spiky (energy) gain at the instant of collision; however, the total (energy) gain is not very large even though the time elapses, because colliding times are finite.

associated electric field is of the order of a few hundred  $\mu\text{V}/\text{cm}$ . This situation would be more realistic, if we were to consider weaker shock waves, such as a blast wave propagating through the universe filled with plasmas and IMF. Additionally, the wave front of the moving cloud must be widespread enough to accelerate the particle to ultrahigh energies.

Attractive features of MTA are summarized in the following. The particle acceleration is continuous and indefinite provided that the trapping condition holds; in that case, the acceleration efficiency is fairly good. Moreover, the MTA provides reasonable values for the estimates of the elapse time and acceleration length that are needed to obtain ultrahigh energies. This situation is similar to that of the shock surfing acceleration.<sup>28,29</sup>

A magnetic neutral sheet and the MTA mechanism could be created anywhere in the universe. For instance, the existence of a magnetic field perpendicular to the galactic plane has been observed in the galaxy NGC4631.<sup>30,31</sup> Colliding galaxies with such perpendicular magnetic fields might present a possibility for generating ultrahigh-energy par-

ticles. In rather low-energy situations, such as a solar flare or the magnetotail of the earth, the MTA mechanism may be a possible candidate for generating energetic particles, because the MNS is considered to play an important role in these phenomena.

In single-step acceleration, when the condition  $\beta_p < 1$  is satisfied, the rate of net gain increases proportionally with  $\beta_p |\beta_{y0}|$ . This situation is similar to the first-order Fermi acceleration mechanism. Furthermore, if this acceleration occurs stochastically between moving clouds, then the second-order Fermi acceleration must be adapted. Nevertheless, in the relativistic region, i.e.,  $\beta_p \approx 1$ , the rate of net gain increases in proportion to a factor of order  $\gamma_p^2$ ; hence this behavior agrees well with the acceleration theory of relativistic blast waves.

The bouncing acceleration might work more effectively in the nonrelativistic region with  $B_0 \ll B_1$ . This situation corresponds to Fermi-type shock acceleration. As the particle is accelerated, multiple collisions with the wave front will be reduced by the relativistic mass effect. Accordingly, this might be a candidate of preacceleration of cosmic rays. As the static magnetic field  $B_0$  approaches zero, the single-step acceleration dominates the bouncing acceleration. In the relativistic region, this acceleration mechanism belongs to the shock surfing acceleration with high Mach number.

In the fundamental features of MTA, the wave damping caused by the high-energy particle acceleration and the power-law energy spectrum might be serious issues therefore careful investigations with respect to the wave-particle interaction will be needed.

## ACKNOWLEDGMENT

The author would like to thank Dr. Harada for his valuable comments and support.

## APPENDIX: PARTICLE ACCELERATION ACROSS STATIC MAGNETIC FIELDS

Particle acceleration across static magnetic fields is easily understood in terms of the induced electromotive force. When a linear rod of wire moves with a speed  $\mathbf{v}$  across a uniform magnetic field  $\mathbf{B}$ , free electrons trapped in the rod experience the Lorentz force  $(q/c)\mathbf{v} \times \mathbf{B}$  and are accelerated along the rod. If the length of the rod is infinitely long and there exists no electrical resistance, then the electrons will be continually accelerated and consequently obtain energy indefinitely. Consider the use of the MNS in place of the linear rod. Many electrons trapped by the MNS will be accelerated in the same way. Furthermore, even if we replace the linear rod with an electrostatic wave, the electrons still will be accelerated because they will be trapped by the potential well of the wave.

Sagdeev and Shapiro<sup>32</sup> have shown the Landau damping of an electrostatic wave in a transverse magnetic field. Under the same field configuration Sugihara and Midzuno<sup>33</sup> have proposed the novel  $\mathbf{v}_p \times \mathbf{B}$  particle acceleration mechanism in the nonrelativistic regime. Dawson *et al.*<sup>34</sup> and Katsouleas and Dawson<sup>35</sup> extended this analysis to the relativistic regime and referred to this acceleration mechanism as Surfa-

tron leading to the shock surfing acceleration. Nishida *et al.*,<sup>36</sup> have performed the first experiment verifying the  $\mathbf{v}_p \times \mathbf{B}$  acceleration process in weakly magnetized plasmas. The MTA mechanism presented here has features similar to those shown by  $\mathbf{v}_p \times \mathbf{B}$  acceleration and Surfatron, however, we note that there exists a remarkable difference between MTA and Surfatron. Namely, the waves used to accelerate particles to high energy. Electromagnetic waves are used in the former, while electrostatic waves are used in the latter. Experimental verification of MTA has been successfully performed by Nishida and co-workers.<sup>36,37</sup> Also, research into the application of MTA in a new type of acceleration device has been developed.

The indefinite acceleration of a particle in electric and magnetic fields that are constant, uniform, and mutually perpendicular has been proposed by Landau and Lifshitz<sup>38</sup> and Jackson.<sup>39</sup> If the magnitude of the electric field is greater than or equal to that of the magnetic field, then the relativistic  $\mathbf{E} \times \mathbf{B}$  acceleration will work effectively. The energy gains and particle trajectories have been calculated in detail by Takeuchi.<sup>40</sup> This mechanism might also be a candidate for the generation of high-energy particles provided that the necessary conditions are satisfied somewhere in the universe

- <sup>1</sup>M. Takeda, N. Hayashida, K. Honda *et al.*, Phys. Rev. Lett. **81**, 1163 (1998).
- <sup>2</sup>M. Nagano and A. A. Watson, Rev. Mod. Phys. **72**, 689 (2000).
- <sup>3</sup>A. V. Olinto, Nucl. Phys. B, Proc. Suppl. **97**, 66 (2001).
- <sup>4</sup>T. Stanev, Nucl. Phys. B, Proc. Suppl. **60B**, 181 (1998).
- <sup>5</sup>L. O'C. Drury, Contemp. Phys. **35**, 231 (1994).
- <sup>6</sup>M. Ostrowski, Astropart. Phys. **18**, 229 (2002).
- <sup>7</sup>E. Fermi, Phys. Rev. **75**, 1169 (1949).
- <sup>8</sup>W. I. Axford, E. Leer, and G. Skadron, *Proceedings of the 15th International Cosmic Ray Conference, Plovdiv, Bulgaria, 13–26 August 1977*, edited by K. Pinkaw (Bulgarian Academy of Science, Sophia, 1977).
- <sup>9</sup>G. F. Krymsky, Dokl. Akad. Nauk SSSR **234**, 1306 (1977).
- <sup>10</sup>A. R. Bell, Mon. Not. R. Astron. Soc. **182**, 147 (1978).
- <sup>11</sup>R. D. Blandford and J. P. Ostriker, Astrophys. J. **221**, L29 (1978).
- <sup>12</sup>J. R. Jokipii, Space Sci. Rev. **86**, 161 (1998).
- <sup>13</sup>L. O'C. Drury, Rep. Prog. Phys. **46**, 973 (1983).
- <sup>14</sup>T. Tanimori, Y. Hayashi, S. Kamei *et al.*, Astrophys. J. Lett. **497**, L25 (1998); **497**, L2 (1998).
- <sup>15</sup>E. Waxman, Phys. Rev. Lett. **75**, 386 (1995).
- <sup>16</sup>M. Sasaki, N. Nagano, and the other Telescope Array Collaborators, *Proceedings of the 27th International Cosmic Ray Conference, Hanburg, Germany, 7–15 August 2001*, edited by R. Schlickeiser (Copernicus Gesellschaft, Katlenburg-Lindau, 2001), p. 873.
- <sup>17</sup>S. Takeuchi, K. Sakai, M. Matsumoto, and R. Sugihara, Phys. Lett. A **122**, 257 (1987).
- <sup>18</sup>S. Takeuchi, K. Sakai, M. Matsumoto, and R. Sugihara, IEEE Trans. Plasma Sci. **PS-15**, 251 (1987).
- <sup>19</sup>S. Kawata, A. Manabe, T. Yabe, S. Takeuchi, K. Sakai, and R. Sugihara, Jpn. J. Appl. Phys., Part 1 **27**, 1980 (1988).
- <sup>20</sup>S. Takeuchi, K. Sakai, M. Matsumoto, and S. Kawata, J. Phys. Soc. Jpn. **59**, 152 (1990).
- <sup>21</sup>P. K. Shukla and A. A. Mamun, Phys. Plasmas **8**, 3126 (2001).
- <sup>22</sup>P. W. Seymour, Aust. J. Phys. **12**, 309 (1959).
- <sup>23</sup>B. U. Ö. Sonnerup, J. Geophys. Res. **76**, 8211 (1971).
- <sup>24</sup>K. Greisen, Phys. Rev. Lett. **16**, 748 (1966); G. T. Zatsepin and V. A. Kuzmin, JETP Lett. **4**, 78 (1966).
- <sup>25</sup>Y. A. Gallant and A. Achterberg, Mon. Not. R. Astron. Soc. **305**, L6 (1999).
- <sup>26</sup>J. Bednarz and M. Ostrowski, Phys. Rev. Lett. **80**, 3911 (1998).
- <sup>27</sup>C. D. Dermer, *Proceedings of the 27th International Cosmic Ray Conference, Hanburg, Germany, 7–15 August 2001*, edited by R. Schlickeiser (Copernicus Gesellschaft, Katlenburg-Lindau, 2001), p. 2039.
- <sup>28</sup>M. Hoshino and N. Shimada, Astrophys. J. **572**, 880 (2002).
- <sup>29</sup>M. Hoshino, Prog. Theor. Phys. Suppl. **143**, 149 (2001).
- <sup>30</sup>E. Hummel, R. Beck, and M. Dahlem, Astron. Astrophys. **248**, 23 (1991).
- <sup>31</sup>S. Takeuchi, *Proceedings of the Magnetodynamic Phenomena in the Solar Atmosphere—Prototypes of Stellar Magnetic Activity, Makuhari, Near Tokyo, 22–26 May 1995*, edited by Y. Uchida *et al.* (Kluwer Academic, Dordrecht, 1996), p. 581.
- <sup>32</sup>R. Z. Sagdeev and V. D. Shapiro, Zh. Eksp. Teor. Fiz. Pis'ma Red. **17**, 387 (1973) [JETP Lett. **17**, 279 (1973)].
- <sup>33</sup>R. Sugihara and Y. Midzuno, J. Phys. Soc. Jpn. **47**, 1290 (1979).
- <sup>34</sup>J. M. Dawson, V. K. Decyk, R. W. Huff, I. Jechart, T. Katsouleas, J. N. Leboeuf, B. Lembege, R. M. Martinez, Y. Ohsawa, and S. T. Ratliff, Phys. Rev. Lett. **50**, 1455 (1983).
- <sup>35</sup>T. Katsouleas and J. M. Dawson, Phys. Rev. Lett. **51**, 392 (1983).
- <sup>36</sup>Y. Nishida, M. Yoshizumi, and R. Sugihara, Phys. Lett. **105A**, 300 (1984).
- <sup>37</sup>N. Yugami, K. Kikuta, and Y. Nishida, Phys. Rev. Lett. **76**, 1635 (1996).
- <sup>38</sup>L. D. Landau and E. M. Lifshitz, in *The Classical Theory of Fields*, Course of Theoretical Physics Vol. 2, 4th ed. (Pergamon, Oxford, 1975), pp. 43–65.
- <sup>39</sup>J. D. Jackson, *Classical Electrodynamics*, 2nd ed. (Wiley, New York, 1975), pp. 571–617.
- <sup>40</sup>S. Takeuchi, Phys. Rev. E **66**, 037402 (2002).